RESEARCH ARTICLE

Retinoid X receptor α downregulation is required for tail and caudal spinal cord regeneration in the adult newt

Sarah E. Walker[1], Rachel Nottrodt[1, 2], Lucas Maddalena[1, 3], Christopher Carter[1, 4], Gaynor E. Spencer[1], Robert L. Carlone[1, *]

1 Department of Biological Sciences, Brock University, Ontario, Canada
2 Department of Geosciences, University of Calgary, Calgary Alberta, Canada
3 Biomedical Sciences, Cambridge University, Cambridge, UK
4 Pre-Health Sciences Department, Niagara College, Welland, Ontario, Canada

Funding: *This study was supported by Natural Sciences and Engineering Council of Canada Discovery Grant to RLC and GES.*

Abstract

Some adult vertebrate species, such as newts, axolotls and zebrafish, have the ability to regenerate their central nervous system (CNS). However, the factors that establish a permissive CNS environment for correct morphological and functional regeneration in these species are not well understood. Recent evidence supports a role for retinoid signaling in the intrinsic ability of neurons, in these regeneration-competent species, to regrow after CNS injury. Previously, we demonstrated that a specific retinoic acid receptor (RAR) subtype, RARβ, mediates the effects of endogenous retinoic acid (RA) on neuronal growth and guidance in the adult newt CNS after injury. Here, we now examine the expression of the retinoid X receptor RXRα (a potential heterodimeric transcriptional regulator with RARβ), in newt tail and spinal cord regeneration. We show that at 21 days post-amputation (dpa), RXRα is expressed at temporally distinct periods and in non-overlapping spatial domains compared to RARβ. Whereas RARβ protein levels increase, RXRα proteins level decrease by 21 dpa. A selective agonist for RXR, SR11237, prevents both this downregulation of RXRα and upregulation of RARβ and inhibits tail and caudal spinal cord regeneration. Moreover, treatment with a selective antagonist for RARβ, LE135, inhibits regeneration with the same morphological consequences as treatment with SR11237. Interestingly, LE135 treatment also inhibits the normal downregulation of RXRα in tail and spinal cord tissues at 21 dpa. These results reveal a previously unidentified, indirect regulatory feedback loop between these two receptor subtypes in regulating the regeneration of tail and spinal cord tissues in this regeneration-competent newt.

***Correspondence to:**
Robert L. Carlone, Ph.D., rcarlone@brocku.ca.

orcid:
0000-0002-5007-2921 (Robert L. Carlone)

doi: *10.4103/1673-5374.233447*

Accepted: *2018-04-09*

Key Words: *retinoid X receptor; spinal cord regeneration; newt; retinoic acid; ependymoglia; retinoic acid receptor*

Introduction

The regeneration of body parts in adult vertebrates is a phenomenon largely restricted to a few species. In particular, zebrafish, as well as urodele amphibians such as axolotls and newts, have been widely used as models for the study of this complex process (Sánchez Alvarado and Tsonis, 2006; Reddien and Tanaka, 2016). In addition to the replacement of lost appendages and many internal organs and tissues, these species, unlike mammals, have the ability to repair and replace damaged spinal cord tissue to produce functional neuronal connections (Tanaka and Ferretti, 2009).

There are many differences between these regeneration-competent species and mammals with respect to their initial responses to trauma and their ability to provide a permissive environment for axonal regrowth. In mammals, in addition to the establishment of an inhibitory glial scar (Silver and Miller, 2004), adult axons exhibit a diminished capacity to regrow after injury (Liu et al., 2011). This is thought to be partly due to diminished all-trans retinoic acid (atRA) signaling *via* a specific subtype of nuclear receptor, the retinoic acid receptor beta (RARβ) (Corcoran et al., 2000, 2002; Yip et al., 2006; Wong et al., 2006; Goncalves et al., 2015).

In adult urodele amphibians, no glial scar formation is seen after injury to the spinal cord (Zukor et al., 2011) and the intrinsic ability of axons to regrow after injury is maintained. Indeed, RA signaling *via* RARβ mediates neurite outgrowth in adult newt spinal cord explants (Dmetrichuk et al, 2005). Furthermore, RARβ expression is maintained, albeit at low levels, in the adult spinal cord and significantly upregulated within ependymoglia within the first 7 days after caudal spinal cord resection (Carter et al., 2011). Inhibition of RARβ signaling with a selective antagonist, LE135, affects vertebral skeletal differentiation and prevents regeneration in larval axolotl tails (Nguyen et al., 2017). LE135 also prevents ependymal tube outgrowth and subsequent tail and spinal cord regeneration in the adult newt (Carter et al., 2011).

Little is known regarding the function of potential heterodimeric partner(s) of RARβ, specifically the family of retinoid X receptors (RXRs), during spinal cord regeneration in urodeles. RXRs are also thought to bind as heterodimers with other nuclear hormone receptors including other RAR subtypes, vitamin D receptors and peroxisome proliferation-activated receptors (PPARs), to name a few (Cunningham and Duester, 2015; DiMasi et al., 2015). RXRs are involved in numerous developmental processes (Maden, 2007; Dollé, 2009; Mark et al., 2009; Duester, 2013), including the early development of motor neurons (Solomin et al., 1998; Luria and Furlow, 2004) and the differentiation of stem cells into glutamatergic and dopaminergic neurons (Simandi et al., 2017; Tsai et al., 2015). Only a few studies, however, have

examined the expression and/or function of RXRs in organ or appendage regeneration (Schrage et al., 2006; Zhelyaznik and Mey, 2006; van Neerven and Mey, 2007). In particular, nothing is known regarding their role in CNS regeneration in regeneration-competent species such as newts or zebrafish.

Our objective in the present study was thus to clone a newt homolog of RXRα and determine its spatial and temporal expression patterns. We also sought to determine its function during the course of caudal spinal cord and tail regeneration in the regeneration-competent adult newt.

Materials and Methods

Animal care and surgery

All experiments and procedures were approved by the Brock University Animal Care Committee. Adult eastern red-spotted newts, *Notophthalmus viridescens*, were utilized in all experiments. Animals were housed in containers of dechlorinated water and fed 3 times a week with liver, brine shrimp and blood worms. Prior to surgery, newts were anesthetized in a bath of 0.1% tricaine methane sulfonate (MS-222, Sigma-Aldrich Canada, Oakville, Ontario, Canada), pH 7.0, for 10 minutes. Amputation of the tail was performed approximately 1 cm caudal to the cloaca, followed by a 10-minute recovery on ice. Amputation of limbs were performed below the elbow. At 7, 14, and 21 days post amputation (dpa), newts were again anesthetised and regenerates were collected.

To determine the cross-reactivity of a custom-made snail RXRα antibody in newt tissues, we also isolated the CNS of the snail, *Lymnaea stagnalis*. For analysis, the CNS was dissected from adult snails with a shell length of 18–20 mm. Animals were anesthetized in 25% Listerine for 2 minutes, then placed in a dissection dish containing saline with 20% gentamicin (antibiotic). Following CNS dissection, 3 CNS were pooled per sample, and were then immediately flash frozen in liquid nitrogen and stored at –80°C.

PCR-based cloning of newt RXR cDNA

RT–PCR was performed on cDNA generated from total RNA extracted from the adult newt CNS. Briefly, reverse transcription was carried out with a mixture of poly A and random hexamer primers according to the iScript cDNA synthesis kit (BioRad, Hercules, CA, USA). cDNA was then amplified with 40 pmol of forward (5′-GGG CTA CCT TCC CAC CCT CAT GT-3′) and reverse primers (5′-GCT GGT GAG GTG CCT CAA GCA TT-3′), based on the *Lymnaea stagnalis* RXR cDNA sequence (Carter et al., 2010). Amplification was performed using an Eppendorf Mastercycler Personal Thermocycler with the following conditions: 3 minutes of denaturation at 95°C, 35 cycles at 95°C for 30 seconds, annealing at 55°C for 30 seconds, and elongation at 72°C for 1 minute. Analysis of the products was carried out on 1% agarose gels in TAE buffer stained with ethidium bromide. Fragments of interest were excised from the gel and cloned into the pGemTEasy vector system (Promega, Madison, WI, USA). Sequencing was performed by Génome Québec (Montréal, Canada) using 3730 xl DNA Analyzer systems from Applied Biosystems (Foster City, CA, USA).

Antibodies

We utilized custom-made *Lymnaea stagnalis* RXR (*Lym*-RXR) and *Notophthalmus viridescens* RARβ (*Nv*RARβ) antibodies, both designed against the predicted 'hinge' regions of each protein. These hinge regions cover residues between the DNA binding domain (DBD) and ligand binding domain (LBD), as described by Carter et al. (2010) for RXR, and Carter et al. (2011) for RAR. In additional experiments, we utilized antibodies against human α-tubulin and chicken vimentin, both provided by the Developmental Studies Hybridoma Bank, University of Iowa (Iowa City, IA, USA).

Western blot analysis

Newt tissue regenerates were collected at 0, 7, 14, and 21 dpa (n = 3 for each time point) and immediately flash frozen in liquid nitrogen. Following homogenization in lysis buffer, samples were centrifuged for 30 minutes at 4°C, and total protein concentrations were determined using the BCA protein assay (Pierce, Rockford, IL, USA). 20 μg of total protein from each sample was run on a 12% polyacrylamide resolving gel, and a 4% polyacrylamide stacking gel for 3 hours at 80 V. Following transfer onto nitrocellulose (Millipore, Oakville, Ontario, Canada), membranes were blocked in 3% nonfat skim milk powder/0.1% Tween20/PBS, shaking for 1-hour at room temperature. Membranes were then incubated in primary antibodies; either 1:2500 *Lym*RXR (Pacific Immunology, Ramona, CA, USA), 1:1000 *Nv*RARβ (Pacific Immunology), or 1:500 anti-α-tubulin (Developmental Studies Hybridoma Bank), overnight at 4°C. The following day, membranes were incubated in the corresponding secondary antibody (1:15,000), Alexa Fluor 680 goat anti-rabbit IgG (Invitrogen), or Alexa Fluor 680 goat anti-mouse IgG (Invitrogen, Carlsbad, CA, USA) for 45 minutes at room temperature. Blots were imaged at 700 nm, using the Odyssey Infrared Imaging system. Three biological replicates and two technical replicates were included for analysis. For LE135- or SR11237-treated samples, 14 μg of protein was utilized for Western blot experiments.

Real-time quantitative polymerase chain reaction (RT-qPCR)

Newt samples were again collected at 0, 7, 14, and 21 dpa, and immediately flash frozen in liquid nitrogen. Tissues were then homogenized, and RNA isolation was performed using the Animal Tissue RNA Purification Kit (Norgen Biotek, Thorold, Ontario, Canada). RNA quality was assessed using a NanoDrop Plus spectrometer (General Electric, Thorold, Ontario, Canada), and samples with a 260/280 ratio above 1.8 were utilized in experiments. Using 500 ng of total RNA, cDNA was synthesized using the iScript cDNA Synthesis Kit (BioRad). Primers for RT qPCR were designed using our partial *N.viridescens* RXR sequence (forward 5′-CAT GTA CAC CGG AAC AGT GC-3′ and reverse 5′- TAG GCA GCC GAG TTC AGT C-3′). Reference genes included α-tubulin (forward 5′-ACT GGA GTC AGG TGG ACG AC-3′; reverse 5′-ATT GAG GGT TGC CTT CAG TG-3′), and caspase-3 (forward 5′-CAA CAG GAC CAC AGC AAA

AG-3′; reverse 5′-AAT CTC CTC CAC TGT CTG CC-3′). RT-qPCR was performed using the BioRad CFX Connect Real-Time detection system (BioRad). For each replicate, no template controls (NTC) and no reverse transcriptase controls (NRT) were utilized according to MIQE guidelines. The resultant data were analyzed using the ΔΔCT method, with all samples normalized to both α-tubulin and caspase-3. For tail regenerates, four biological replicates were utilized, while three biological replicates were used for limb samples.

Immunofluorescence staining

Tail tissues were collected at 0 and 21 dpa, then fixed for 24-hour in 4% paraformaldehyde at 4°C. Tissues were decalcified for 24-hours in 10% EDTA (Sigma), followed by a graded series of sucrose washes (10%, 20%, 30%) for 30 minutes with rotation at room temperature. Samples were left rotating in 30% sucrose at 4°C overnight, then stored in 30% sucrose/optimal cutting temperature compound (OCT) (VWR, Mississaugua, Ontario, Canada). 15 μm tissue sections were cut using a Cryomicrotome FSE (Thermoscientific), and collected on Superfrost Plus (VWR) imaging slides. To begin immunostaining, slides were washed for 10 minutes in PBS and permeabilized in 0.1% Triton-X/PBS for 30 minutes at room temperature. Tissues were next blocked in 5% normal goat serum for 1 hour, followed by incubation in the appropriate primary antibodies overnight at 4°C. For double staining, sections were simultaneously incubated in either RXR (1:50) and Vimentin (1:100) (Developmental Studies Hybridoma Bank), or with *Nv*RARβ (1:50) and Vimentin (1:100) antibodies, overnight at 4°C. Negative controls omitted the addition of a primary antibody. The following day, slides were incubated in secondary antibody, Alexa Fluor-488 goat anti-rabbit (for RXR and *Nv*RARβ) (Invitrogen) for 2-hour at room temperature. Samples were then washed in 0.1% Triton-X/PBS, followed by a second incubation in secondary antibody, Alexa Fluor-594 goat anti-mouse (Invitrogen) for vimentin, again at room temperature for 2-hour. Tissue sections were then washed in 0.1% Triton-X/PBS, and counterstained with 4′-6′-diamindino-2-phenylindole (DAPI) (Sigma) for 2 minutes. Slides were mounted in anti-fade Fluorosave mounting media (Sigma), and imaged using a confocal microscope, as described below.

Immunofluorescent imaging

Immunofluorescent images of fixed tissue sections were obtained using a Zeiss Axio Observer.Z1 inverted light/epifluorescence microscope (Zeiss Canada, North York, Ontario, Canada) equipped with ApoTome.2 optical sectioning, Plan-Apochromat 63x/1.40NA oil DIC M27 and 20x/0.8NA M27 objective lenses, and a Hamamatsu ORCA-Flash4.0 V2 digital camera (Hammamatsu, Hammamatsu City, Shizuoka, Japan). Fluorescence illumination was achieved *via* an X-Cite 120LED light source. Alexa-Flour 488 signal was detected using excitation and emission wavelength filter sets of 450–490 nm and 500–550 nm, respectively (Zeiss Item# 411003-0004-000), with set excitation and emission wavelengths of 488 nm and 509 nm, respectively. Alexa-Fluor 594 signal was detected using excitation and emission wavelength filter sets of 540–602 nm and 590–660 nm, respectively (Zeiss Item# 411003-0010-000), with set excitation and emission wavelengths of 587 nm and 610 nm, respectively. DAPI signal was detected using excitation and emission wavelength filter sets of 335–383 nm and 420–470 nm, respectively (Zeiss Item# 411003-0002-000), with set excitation and emission wavelengths of 353 nm and 465 nm, respectively. In samples in which RXR expression was downregulated, spatial protein localization was determined by increasing camera exposure times. Z-stack slices were taken at 0.25–0.3 μm intervals and were rendered into 2D maximum intensity projections using the "extended depth of focus" processing tool of Zeiss Zen 2 (blue edition) microscopy software.

SR11237 and LE135 treatments

Following amputation, animals were maintained in dechlorinated water containing either 1×10^{-6} M SR11237 (RXR pan-agonist, Sigma), 1×10^{-6} M LE135 (RARβ antagonist, Tocris, (Bristol, UK), or 0.01% DMSO (vehicle control). For SR11237 and DMSO-treated samples, newt tail regenerates were imaged at 7, 14, and 21 dpa under a dissecting microscope, using a Nikon DS-U2 camera equipped with NIS Elements software. At 21 dpa, SR11237 (n = 7), LE135 (n = 3) and DMSO (n = 7) regenerates were collected and flash frozen on liquid nitrogen for western blot analysis.

Histological analysis

Following amputation, tissues were fixed overnight in 10% neutral buffered formalin, and decalcified in 10% EDTA (Sigma). The next day, regenerates were dehydrated in a series of ethanol dilutions and cleared overnight in methyl salicylate (Fisher). Tissues were next infiltrated with molten paraffin at 80°C and embedded in paraffin blocks. 15 μm sections were obtained and placed on Superfrost Plus (VWR) slides. Following collection, sections were deparaffinised in xylene for 3 minutes, then rehydrated using a series of diluted ethyl alcohol washes with a final incubation in distilled water for 3 minutes. Tissues were next stained in 1% alcian blue (Sigma)/3% glacial acetic acid for 30 minutes, followed by a 0.1% Fast Red Nuclear Dye (Sigma) stain. Finally, sections were dehydrated in a series of ethyl alcohol washes, and incubated in xylene for 3 minutes. Slides were imaged using a dissecting microscope equipped with a Nikon DS-U2 camera (Tokyo, Japan) and NIS Elements Software (Mississaugua, Ontario, Canada).

Statistical analyses

Data were analyzed using Graphpad Prism, Version 7.00 for Mac OS X (La Jolla, CA, USA), and values were expressed as the mean ± SEM. Statistical analyses were performed using a one-way analysis of variance (ANOVA), followed by Tukey's *post-hoc* test. For statistical analyses of newt tail length following treatment with SR11237 or DMSO, a two-way repeated measures ANOVA was performed, followed by Sidak's multiple comparisons test. For all analyses, a P value less than 0.05 was considered to be statistically significant.

Results

Cloning of partial *Nv*RXRα sequence

Our first objective was to clone a newt homolog of RXRα using a PCR-based approach. We obtained a partial cDNA clone and chose to compare the amino acid sequence of the newt RXR to that of the human (*Homo sapiens*), as well as to regeneration-competent species, such as the zebrafish (*Danio rerio*) and the snail (*Lymnaea stagnalis*). Our comparison to the snail was useful, since in subsequent Western blot analyses, we utilized an antibody produced against the snail RXRα that cross-reacted with the newt antigen. There is a high degree of similarity between the newt, human, zebrafish and snail DNA- and ligand-binding domains of the RXR protein (**Figure 1**). Within the DNA-binding domain, the newt RXRα sequence (*Nv*RXR) shares a 92% identity to the human RXRα (*homo sapiens* RXRα (*Hs*RXR), accession No. AAI10999), 94% identity to the zebrafish RXRα (*Danio rerio* RXR (*Dr*RXR), accession No. AAC59720) and 85% identity to the snail RXR (*Lym*RXR, accession No. AAW34268). In the ligand-binding domain, the *Nv*RXR sequence shares 87% identity to human, 84% identity to zebrafish, and a 76% identity to *Lymnaea*.

RXRα mRNA levels significantly increase in regenerating tissues during the first 21 days, following amputation of both limb and tail

In many cases, RAR and RXR proteins have been shown to heterodimerize and bind to DNA response elements to induce changes in gene expression (Leid et al., 1992; reviewed by Maden, 2002). In a previous study on RARβ expression, Carter et al. (2011) showed an up-regulation in mRNA and protein levels during the first 21 days of tail regeneration in the adult newt. Thus, we sought to examine whether similar phenomena would be seen in newt RXRα transcript and protein levels.

We first examined RXRα mRNA levels using Q-PCR during both limb and tail regeneration. Transcript abundance was examined at the time of amputation (day 0) and at 7, 14 and 21 days post amputation (dpa). We found that RXRα mRNA was significantly upregulated over time in limb tissues, when compared to levels measured at day 0 ($F_{(3,8)}$ = 11.16; P = 0.0031; **Figure 2A**). Similarly, in tail regenerates, RXRα mRNA was significantly upregulated over time ($F_{(3,8)}$ = 6.74; P = 0.0064; **Figure 2B**), showing higher levels at both 14 and 21 dpa, compared to day 0.

RXRα protein is significantly downregulated by 21 dpa in both limb and tail tissues

After identifying increased RXRα mRNA levels during 21 days of newt limb and tail regeneration, we next wanted to determine whether this expression pattern was also reflected at the protein level. Using a custom-made snail (*Lymnaea stagnalis*) RXR antibody (Carter et al., 2010), we were able to demonstrate cross-reactivity with newt tail and limb tissues (**Figure 3A**). The *Lym*RXR antibody cross-reacted with a ~47 kDa protein in all examined tissues from the adult newt, including tissue samples taken from the testes and brain (**Figure 3B**). This molecular weight corresponds to that of the snail RXR (~47 kDa; Carter et al., 2010), as well as with the RXR of other species, such as human (~52 kDa; Nickkho-Amiry et al., 2012) and zebrafish (~47 kDa, UniProt).

Utilizing this antibody, we were able to examine the temporal changes in newt RXRα protein expression during the first 21 dpa in regenerating limb and tail tissues. Interestingly, RXRα protein was found to be significantly downregulated over the first 21-days of regeneration in both limb ($F_{(3,20)}$ = 21.92; P < 0.0001) and tail tissues ($F_{(3,20)}$ = 13.12; P < 0.0001) (**Figure 3C**, **D**). In the limb, RXRα was significantly downregulated at 7 dpa (P = 0.001), 14 dpa (P < 0.0001) and 21 dpa (P < 0.0001; **Figure 3C, E**), when compared to expression levels at day 0. There was also a significant downregulation between 7 dpa and 21 dpa (P = 0.0258).

Similar changes were found in tail regenerates, as RXRα was significantly downregulated at 21 dpa when compared to day 0 (P = 0.0016; **Figure 3D, F**). A significant downregulation was also shown at 21 dpa when compared to expres-

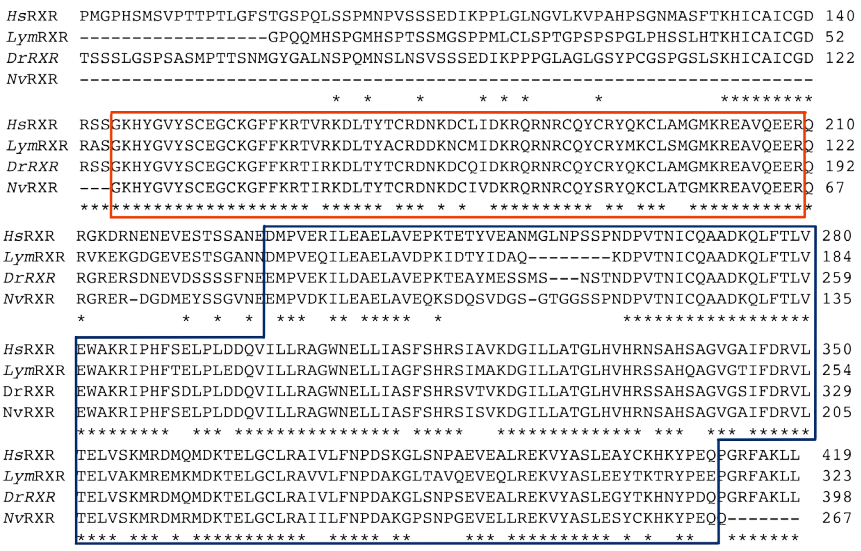

Figure 1 Sequence alignment of the *Notophthalmus viridescens* partial retinoid X receptor (RXR) amino acid sequence (*Nv*RXR, accession No. ADI24671).

Multiple sequence alignment with the full-length *Homo sapiens* RXRα (*Hs*RXR, accession No. AAI10999), *Lymnaea stagnalis* RXR (*Lym*RXR, accession No. AAW34268) and *Danio rerio* RXR (*Dr*RXR, accession No. AAC59720), shows a high degree of similarity within the DNA binding domain (DBD; red box), and the ligand-binding domain (LBD; blue box). Asterisks represented conserved amino acids across all four samples.

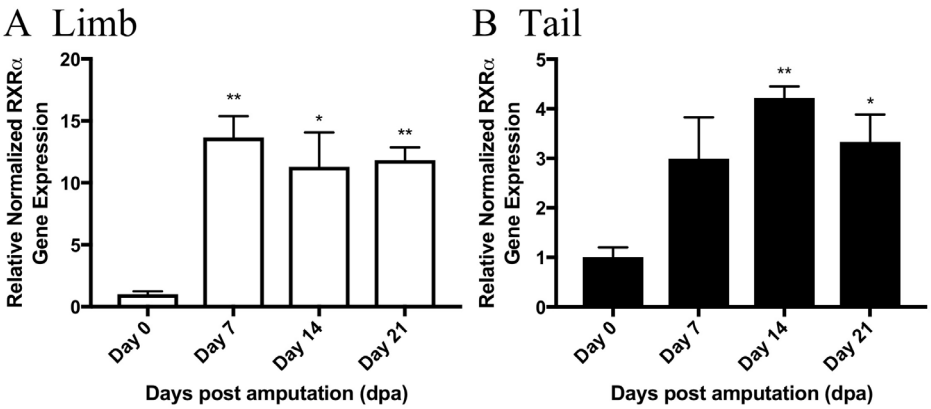

Figure 2 *Nv*RXRα gene expression is significantly upregulated during limb and tail regeneration.
Q-PCR indicates a significant increase in RXRα transcript levels by 7 days post-amputation (dpa) in regenerating limb (A) and by 14 dpa in regenerating tail tissues (B). All samples were compared to day 0 samples, and normalized to both caspase-3 and α-tubulin transcript expression. Data were expressed as the mean ± SEM, and analyzed using a one-way analysis of variance. $*P < 0.05$, $**P < 0.01$, *vs.* day 0.

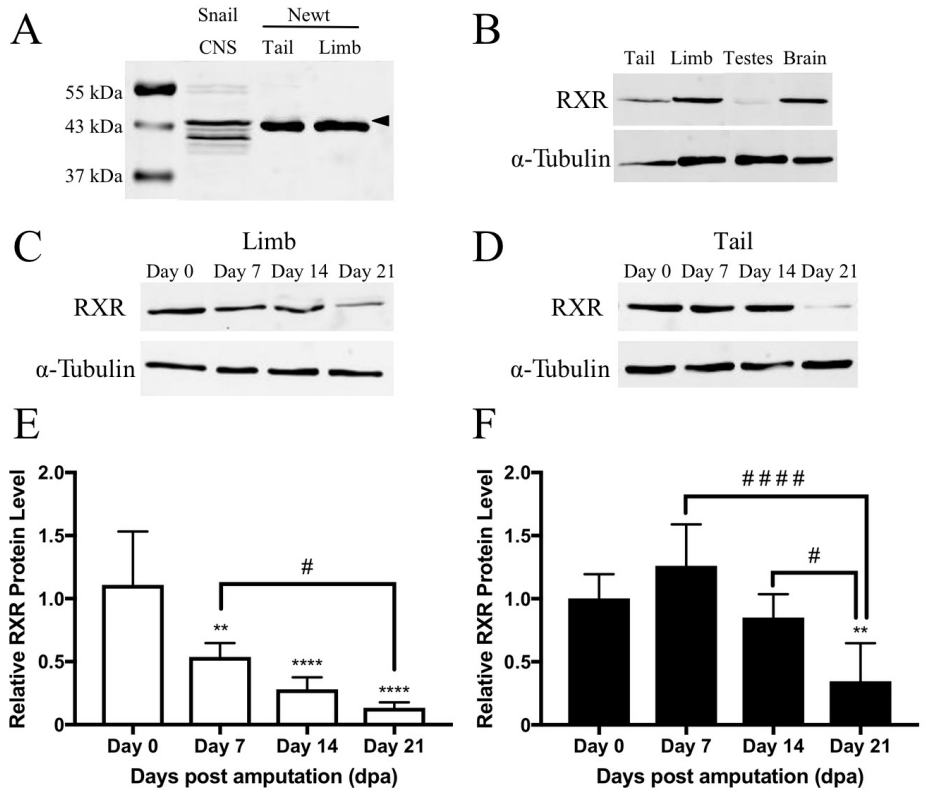

Figure 3 Retinoid X receptor (RXR)α protein expression in the adult newt.
(A) Western blot demonstrating cross-reactivity of the *Lymnaea stagnalis* RXR (*Lym*RXR) antibody in newt tissues, as a similar sized band at ~47 kDa (black arrow) is shown in both newt limb and tail tissues, as in the snail central nervous system (CNS). (B) The *Lym*RXR antibody also reacts in additional newt tissues, including the testes and brain. (C, D) Western blot analysis demonstrates a significant decrease in RXR protein expression across the entire 21 days of newt limb regeneration (C), while a significant down-regulation in the tail is detected at 21 days (D). (E, F) The mean band densities at 7, 14 and 21 days post-amputation (dpa) from limb (E) and tail (F) are represented relative to the average band density of day 0, and normalized to the densities of the loading control, α-tubulin. Data were expressed as the mean ± SEM, and analyzed using a one-way analysis of variance. $**P < 0.01$, $****P < 0.0001$, *vs.* day 0; $\#P < 0.05$, $\#\#\#\#P < 0.0001$.

sion levels at 7 dpa ($P < 0.0001$) and 14 dpa ($P = 0.015$).

RXRα protein exhibits a non-overlapping spatial pattern of expression in comparison to RARβ during tail and caudal spinal cord regeneration

We have previously shown that RARβ protein levels increased during tail regeneration (Carter et al., 2011), whereas in this study, we found that RXRα protein levels decreased after tail amputation. We were next interested in examining the precise tissue and cellular localization of RXRα at various time points following tail amputation, and to compare this localization with that of RARβ. As we previously studied the localization of RARβ in regenerating newt tail and spinal cord (Carter et al., 2011), we thus restricted our analysis of RXRα to these same tissues.

We examined the spatial distribution of RXRα at two time points, day 0 (immediately following amputation) and 21 dpa (the time point showing the greatest reduction of this protein in the tail regenerate). We also re-examined the cellular distribution of RARβ at similar stages from the same tissues. **Figure 4** illustrates receptor localization in transverse sections of the regenerating tail, whereas **Figure 5** illustrates receptor expression in sagittal sections. The saggittal sections were taken both rostral and caudal to the amputation plane in order to compare receptor expression in both the stump and regeneration blastema, respectively.

Interestingly, the cellular domains of RARβ and RXRα expression were very different, with no apparent overlap in the tail or spinal cord. Furthermore, neither receptor appeared to be located within the nuclei of any cells, at either day 0 or 21 dpa (**Figures 4** and **5**). At 0 dpa, RARβ was expressed within ependymoglia (eg) (**Figure 4Ai–ii**) and in meningeal

cells, as seen in our previous study (Carter et al., 2011), and was co-localized with vimentin within ependymoglia (**Figure 4Aiii–iv**). RXRα, on the other hand, was abundant within the sub-ependymal cells, surrounding the ependymoglia (**Figure 4v–vi**), and did not appear to be co-localized with vimentin (**Figure 4Avii–viii**).

At 21 dpa, RARβ was strongly expressed in fibrous processes (**Figure 4Bi**) within the regenerated axons and was seen within occasional vimentin-positive cells (**Figures 4Biii–iv, 5Bii**). Again, this cellular distribution is reminiscent of that seen in our earlier work. Curiously, RXRα was widely dispersed, often appearing as cytoplasmic punctae throughout the spinal cord. However, it still did not co-localize with vimentin-positive cells, either in the rostral stump tissue, or in the more caudal regeneration blastema (**Figures 4Bvii–viii, 5Biv, Civ**).

A RXR pan-agonist, SR11237, inhibits tail and caudal spinal cord regeneration

We next aimed to determine the function of RXRα protein downregulation during spinal cord regeneration. We attempted to reverse this downregulation by incubating newts in a bath containing either an RXR pan-agonist (1×10^{-6} M SR11237), or DMSO (0.01% v:v; vehicle control). We first examined the extent of tail regeneration and found a significant interaction between treatment and time ($F_{(2,22)} = 32.68$; $P < 0.0001$). Specifically, newts incubated in SR11237 exhibited a significant decrease in the length of the tail regenerate, when compared to DMSO-treated controls at 21 dpa ($P < 0.0001$; **Figure 6A, B**). No changes in tail length were shown at 7 dpa ($P = 0.9414$) or 14 dpa ($P = 0.9947$). Western blotting also confirmed that the decrease in RXRα expression normally seen at 21 dpa (DMSO-treated controls) was reversed in SR11237-treated animals (**Figure 6C**). Interestingly, this RXR agonist also prevented the normal accumulation of RARβ seen at 21 dpa in DMSO treated regenerates (**Figure 6C**). Thus, it appears that both downregulation of RXRα and upregulation of RARβ between 0 dpa and 21 dpa, albeit in different cells, is required for tail and caudal spinal cord regeneration in this species.

SR11237 treatment inhibits both ependymal tube and cartilaginous rod outgrowth from the stump tissues

Histological examination of sagittal sections of tail regenerates at 21 dpa revealed that treatment with SR11237 appeared to prevent both ependymal tube elongation and cartilaginous rod formation, beyond the original plane of amputation (**Figure 7B**). In addition, instead of blastemal mesenchyme cell proliferation and accumulation beneath the wound epithelium, as seen in control regenerates (**Figure 7A**), fibrocellular scar tissue appeared caudal to the plane of amputation in SR11237-treated tails (**Figure 7B**). Interestingly, these histological effects observed with the RXR pan-agonist, closely mimic those seen previously with a similar bath application of an RARβ antagonist, LE135, between 0 and 21 dpa (Carter et al., 2011).

The expression levels of RARβ and RXRα proteins may be indirectly interdependent during tail and caudal spinal cord regeneration

Since the SR11237-induced up-regulation of RXR signaling produced similar inhibitory effects on tail and caudal spinal cord regeneration as previous treatment with a RARβ antagonist (LE135) (Carter et al., 2011), our next aim was to determine whether LE135 would also induce an upregulation of RXRα protein at 21 dpa. Indeed, we found that newts bathed in LE135 demonstrated a significant upregulation of RXRα protein after 21-day, when compared to DMSO-treated controls ($P = 0.0002$) (**Figure 8A, B**). Interestingly, LE135 treatment restored RXRα levels to those expressed in unamputated tail tissues (**Figure 8A, B**). We also examined the expression of RARβ in these same tissue samples, and confirmed its abundance in DMSO-treated controls, followed by a significant downregulation in LE135-treated tail regenerates at 21 dpa ($P < 0.0001$). These results, together with those in response to the RXR agonist treatment described above, suggest a possible regulatory interdependence between RXRα and RARβ during spinal cord regeneration.

Discussion

In previous work examining the regenerating newt tail and spinal cord, both RARβ mRNA and protein were shown to significantly increase in the caudal spinal cord following injury (Carter et al., 2011). Since RARβ often acts as a heterodimeric partner with RXRα in numerous cell types (Mangelsdorf et al., 1992; Lefebvre et al., 2010), we now examined the spatial and temporal domains of RXRα expression after tail amputation.

RXRα protein levels decrease after transection of the tail and caudal spinal cord and may be regulated post-transcriptionally

In this study, we cloned a partial RXRα sequence from the newt, *Notophthalmus viridescens*, and provided the first evidence for a post-transcriptionally regulated downregulation of RXRα within the transected spinal cord of a regeneration-competent species. This decrease in RXRα protein occurs at a time point between 14 and 21 dpa. We have also demonstrated that this downregulation is necessary for the outgrowth and integrity of a posterior cartilaginous rod as well as for the growth and posterior extension of an ependymal tube. Finally, we provide evidence that the expression of RARβ and RXRα may be inversely interdependent during the first 21 dpa. Inhibition of RARβ signaling led to an accumulation of RXRα, while agonist induced accumulation of RXRα inhibited the normal upregulation of RARβ by 21 dpa, despite apparent non-overlapping spatial expression domains.

In the sciatic nerve of the rat (a regeneration-competent nerve), both RARβ and RXRα mRNAs and proteins were previously found to increase following injury (Zhelyaznik and Mey, 2006). RXRα levels were upregulated in nerves and macrophages as early as 4 days post-crush injury, although similar increases were not seen in nerves post-transection. Contrary to this finding, in a regeneration-incompetent

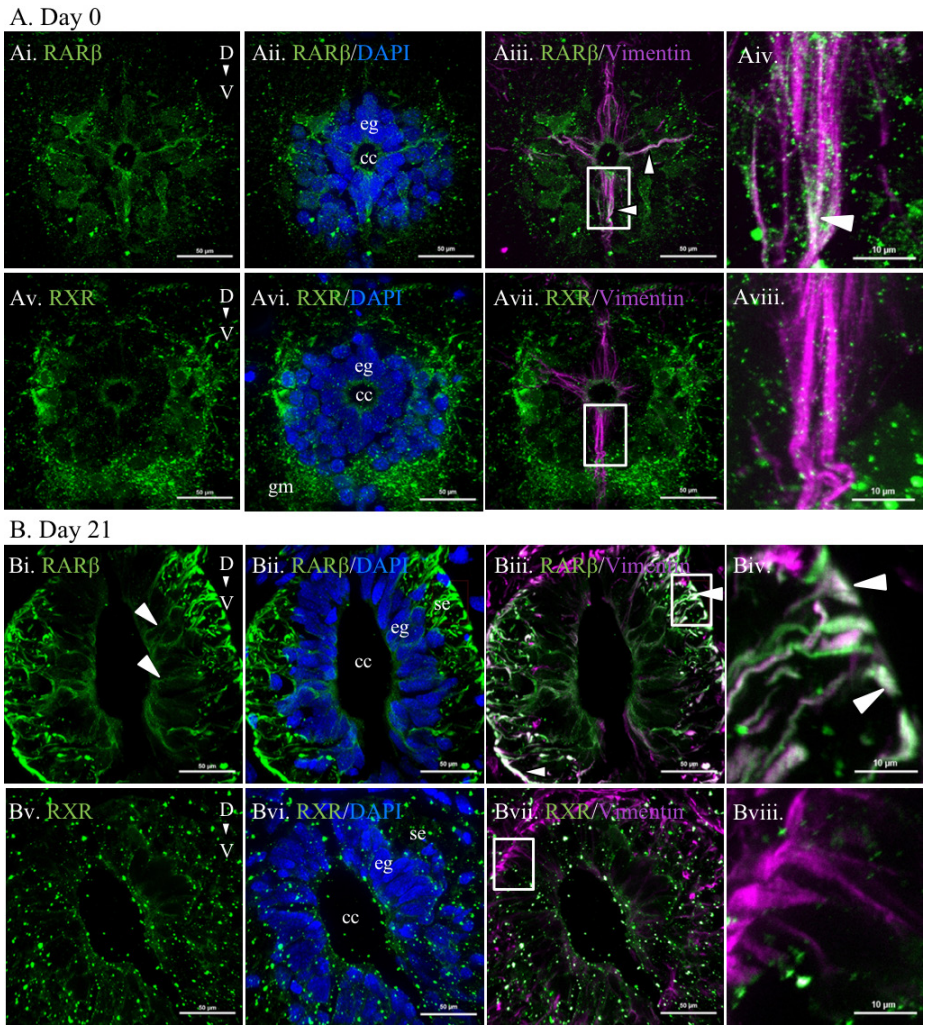

Figure 4 Spatial expression of retinoic acid receptor (RAR)β and retinoid X receptor (RXR)α protein in the spinal cord of day 0 and day 21 regenerates.
(A) Immunoflourescent images of RARβ (Ai–iv) and RXRα (Av–viii) protein in day 0 spinal cords. White boxes indicate regions of interest that are shown at a higher magnification in Aiv and Aviii, and white arrowhead indicates co-localization with vimentin. (B) RARβ (Bi–iv) and RXRα (Bv–viii) in the regenerating cord blastema at 21 days post-amputation (dpa). White boxes indicate regions of interest that are shown at a higher magnification in Biv and Bviii, and white arrowheads indicate co-localization with vimentin. In Bi, white arrowheads indicate RARβ expression in fibrous processes. Scale bars for images set at 50 μm and 10 μm for regions of interest. D–V indicates direction of dorsal to ventral axes. cc: Central canal; eg: ependymoglia; se: subependymal cells; gm: grey matter.

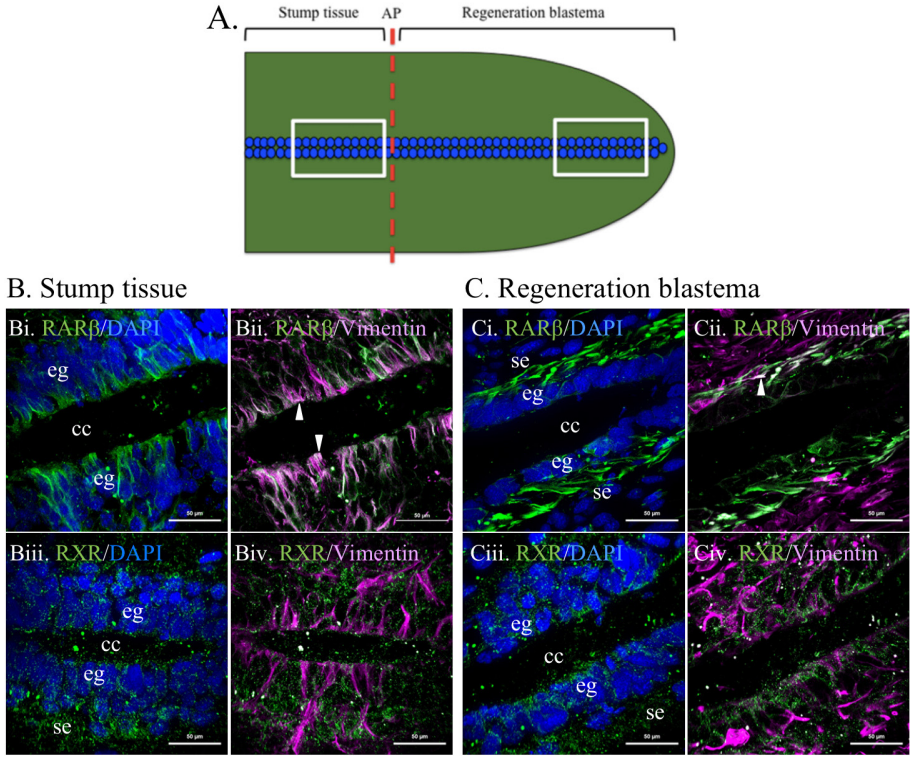

Figure 5 Expression of retinoic acid receptor (RAR)β and retinoid X receptor (RXR)α in the spinal cord of day 21 stump tissue and the distal regenerate.
(A) Image depicts the structure of a regenerating newt tail. Red line marks the amputation plane (AP), which separates the stump tissue (left) from the regeneration blastema (right). Blue circles represent the ependymal cells of the spinal cord. White boxes indicate approximate area of immunofluorescent images. (B) Localization of RARβ and RXRα in day 21 stump tissues. White arrowheads indicate co-localization with vimentin. (C) RARβ and RXRα protein expression in the distal regeneration blastema at 21 days post-amputation (dpa). White arrowhead indicates area of RARβ-vimentin co-localization. Scale bars for all images set at 50 μm. cc: Central canal; eg: ependymoglia; se: subependymal cells.

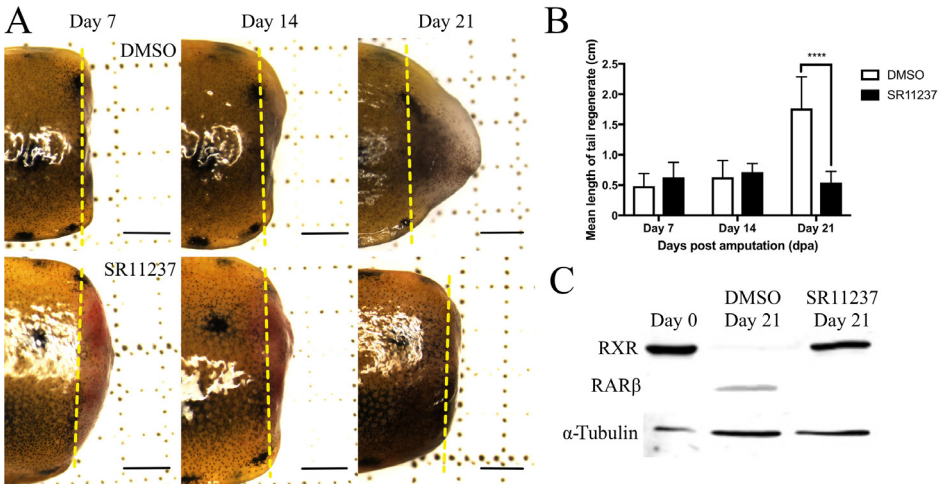

Figure 6 Bath application of a retinoid X receptor (RXR) pan-agonist, SR11237, significantly inhibits tail regeneration.
(A) Representative images at various stages of tail regeneration of newts bathed in 1 × 10^{-6} M SR11237, in comparison to the vehicle control (0.01% DMSO). Scale bars: 1 cm. (B) The mean length of SR11237-treated tail regenerates was significantly decreased in comparison to DMSO-treated controls at 21 days post-amputation (dpa). Data were expressed as the mean ± SEM, and analyzed using a two-way analysis of variance. ****P < 0.0001. (C) Representative western blot of RXRα and retinoic acid receptor (RAR)β protein from SR11237-treated and DMSO-treated (control) tail regenerates at 21 dpa. α-Tubulin served as the loading control.

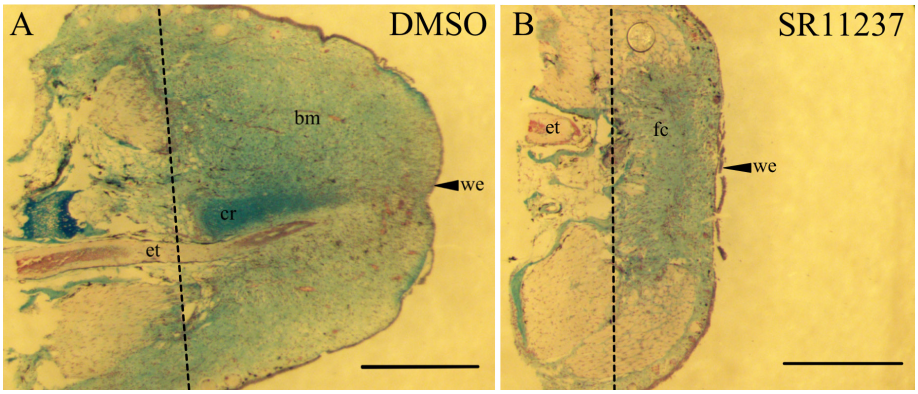

Figure 7 Treatment with SR11237 inhibits ependymal tube outgrowth and promotes scarring.
(A) Representative mid-sagittal section of a 21 days post-amputation (dpa) tail regenerate bathed continuously in 0.01% DMSO. (B) A similar mid-saggittal section of a 21 dpa tail regenerate bathed in 1 × 10^{-6} M SR11237. Dotted lines represent original plane of amputation. et: Ependymal tube; cr: cartilaginous rod; we: wound epithelium; bm: blastemal mesenchyme; fc: fibrocellular scar. Scale bars: 1 cm.

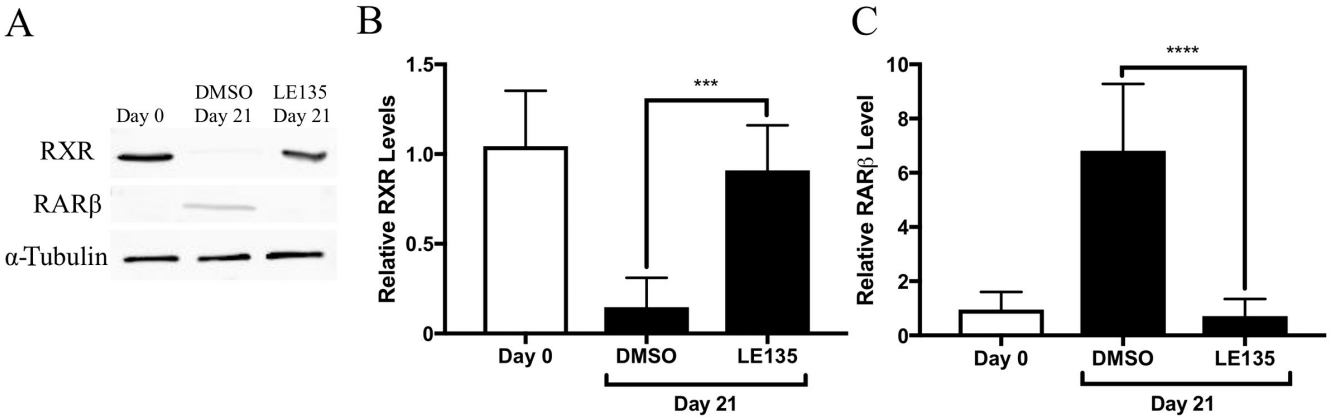

Figure 8 Retinoid X receptor (RXR)α is upregulated in regenerating tails when retinoic acid receptor (RAR)β is pharmacologically inhibited.
(A) Western blot of RXRα and RARβ protein from LE135-treated regenerates at 21 days post-amputation (dpa). (B) RXRα expression is significantly upregulated when compared to DMSO-treated controls at 21 dpa. (C) RARβ is significantly inhibited in LE135 samples at 21 dpa, compared to DMSO controls. Values are represented relative to the average band density of day 0, and normalized to α-tubulin. Data were expressed as the mean ± SEM, and analyzed using a one-way analysis of variance. ***P = 0.0002, ****P < 0.0001.

preparation (adult rat spinal cord), Schrage et al. (2006) determined that RXRα protein, though present in the uninjured cord, decreases over the first 14 days post-crush injury. This decrease in RXRα is accompanied by a translocation of the receptor from the cytosol into the nucleus in neurons, microglia, and macrophages following injury.

Based on the above findings in rats, we hypothesized that in our regeneration-competent newt spinal cord and tail model, RXRα would be increased in parallel with RARβ. However, we found an overall decrease in RXRα protein by 21 dpa, though paradoxically, RXR mRNA levels increased over the same time period, perhaps due to post-transcriptional regulation. Indeed, there is precedence in the literature for differential post-transcriptional control of RXRα in a variety of brain and spinal cord regions of the adult mouse (Krezel et al.,1999). In that study, RXRα mRNA was shown to be abundant in regions of the spinal cord which completely lacked corresponding protein expression. On

the other hand, RARβ mRNA was only present in those areas that contained RARβ protein. Thus, it appears that post-transcriptional control of RXRα, but not RARβ, might represent a conserved mechanism for differential regulation of the abundance of the receptor subtypes in uninjured and injured CNS tissue.

Numerous post-transcriptional regulatory mechanisms may be regulating RXRα expression in these tissues. MicroRNAs (miRNAs), *via* control of mRNA translation, have previously been shown to modulate RXRα expression in a variety of cell types. For example, in hepatic stellate cell cultures, miR-27a and 27b target RXRα mRNA, to decrease cell proliferation (Ji et al., 2009). Similarly, a pro-apoptotic miRNA, miR-128, has been shown to target RXRα mRNA, in turn modulating cholesterol homeostasis in HepG2, MCF7 and HEK293T cell cultures (Adlakha et al., 2013). Interestingly, these studies both described how regulation of RXRα mRNA by miRNAs, corresponded to a decrease in cell proliferation. Twenty-one dpa in the regenerating newt tail represents a stage of extensive differentiation and decreased cell proliferation (Iten and Bryant, 1976). Thus, the downregulation of RXRα protein by 21 dpa in the newt, may result from increased miRNA activity on RXRα mRNAs, to promote decreased cell proliferation with a concomitant increase in differentiation. In limb tissues, extensive differentiation occurs much earlier (by 6 dpa) in the regeneration blastema (Iten and Bryant, 1973). These different time points correspond to the findings of our study; that is, a significant decrease in RXRα protein was shown in the limb by 7 dpa, but was not shown in the tail and caudal spinal cord until 21 dpa. Taken together, a downregulation of RXRα, possibly by miRNAs, or other post-transcriptional regulatory mechanisms, may be required to limit cell proliferation and promote cell differentiation during regeneration.

RXRα and RARβ proteins are expressed in different domains within the regenerating tail and spinal cord

In tail tissue at the time of amputation, as well as in proximal stump tissue at 21 dpa, RXRα protein expression was found in a diffuse pattern, with occasional puncta within the cytoplasm of both the ependymal layer and the more peripheral sub-ependymal (vimentin-negative) cells. Unlike in the rat (Schrage et al, 2006), we saw no evidence of translocation of RXRα from the cytoplasm to the nuclei in any cells as a consequence of injury to the tail and caudal spinal cord. As we have previously reported (Carter et al., 2011), RARβ protein is significantly upregulated in the caudal spinal cord by 21 dpa and is primarily localized within the cytoplasm of vimentin-positive radial ependymoglial cells in stump tissues. At 21 dpa, while some expression in the distal tail blastema is still associated with radial glial cells, RARβ expression can also be seen in the cytoplasm of newly formed neurons in the regenerating spinal cord. However, as with the RXRα, no evidence of nuclear translocation of RARβ is seen.

The lack of any apparent tissue or cellular overlap of the RXRα and RARβ receptors, strongly argues against their involvement as heterodimeric partners in directly regulating gene expression during regeneration. Indeed, their extranuclear localization in spinal cord cells, both before and after injury, is supportive of a non-canonical role for these receptor sub-types. The traditional view of retinoid signaling has held that in the absence of ligands such as atRA or 9-cis RA, these receptors reside in the nucleus and ordinarily interact with transcriptional co-repressors that prevent gene expression (Di Masi et al., 2015). Ligand binding then alters the conformation of these complexes and can affect their intracellular localization and/or their relative affinities for co-activators or co-repressors, resulting in transcription of target genes (Di Masi et al., 2015).

More recently, evidence is mounting for an alternative, extranuclear role for both RARs and RXRs, that serves to highlight the extreme complexity of retinoid signaling (Al Tanoury et al., 2013; Piskunov et al., 2014). In hippocampal neurons, RARα has been shown to associate with a subset of mRNAs and RNA-binding proteins in dendritic RNA granules (Chen et al., 2008; Maghsoodi et al., 2008). In response to RA, this extranuclear RARα promotes rapid local translation of a post-synaptic glutamate receptor, GluR1, which subsequently contributes to synaptic plasticity (Aoto et al., 2008). RARs and RXRs have also been shown to be present in both frog and snail growth cones, where there is evidence that they may mediate the axonal guidance effects of exogenous RA, at least *in vitro* (Carter et al., 2010, 2015, Rand et al., 2017).

Two interesting and unexpected findings in this study were 1) that inhibition of RARβ signaling with a selective antagonist (LE135), led to an increase in RXRα protein levels at 21 dpa in tail regenerates, and 2) that a selective RXR agonist (SR11237) treatment also abolished the normal upregulation of RARβ expression seen by 21 dpa. In control tail regenerates by 21 dpa, RARβ expression is strong in differentiated neuronal fibers associated with the regenerating spinal cord. Alternatively, RXRα staining is greatly diminished globally and diffuse in the cytoplasm of both ependymal cells lining the central canal and in subependymal cell cytoplasm. Since both LE135 and SR11237 were continuously present in the bath immediately after amputation of the tail, it is difficult to speculate on possible interactions *in vivo* between the receptor subtypes, genomic response elements and/or translation control components that would result in an increase in RXRα and decrease in RARβ at 21 dpa. It does however, appear that an upregulation of RARβ and concomitant downregulation of RXRα, sometime between 14 and 21 dpa is essential for regeneration of the tail and caudal spinal cord. These changes are occurring within the posterior spinal cord in non-overlapping cellular domains, and appear to be necessary for differentiation of neurons, extension of a cartilaginous rod beyond the original plane of amputation as well as posterior extension of the ependymal tube. It will be an interesting challenge to dissect the interplay between these retinoid signaling pathways *in vivo*, and to develop a more thorough understanding of the factors and cell types involved in the establishment of a permissive environment for spinal cord regeneration in this species.

Acknowledgments: *The authors acknowledge Dr. Jeff Stuart for assistance with the confocal microscopy and the Natural Sciences and Engineering Research Council of Canada for funding this project.*

Author contributions: *Conception and design, literature search, data acquisition, experimental studies, data analysis, statistical analysis, manuscript preparation, manuscript editing, manuscript review: SEW. Conception and*

design, experimental studies, manuscript editing and review: RN. Data acquisition and manuscript editing and review: LM. Experimental studies, data acquisition, manuscript editing and review: CC. Data analysis, statistical analysis, manuscript editing and review: GES. Conception and design, literature search, manuscript preparation, editing and review: RLC.

Conflicts of interest: *The authors declare no conflicts of interest.*

Financial support: *This study was supported by Natural Sciences and Engineering Council of Canada Discovery Grant to RLC and GES.*

Institutional review board statement: *The study protocol was approved by the the Brock University Animal Care Committee.*

Data sharing statement: *Datasets analyzed during the current study are available from the corresponding author on reasonable request.*

Plagiarism check: *Checked twice by iThenticate.*

Peer review: *Externally peer reviewed.*

Open peer reviewer: *Luciana P. Cartarozzi, University of Campinas - UNICAMP, Brazil.*

References

Adlakha YK, Khanna S, Singh R, Singh VP, Agrawal A, Saini N (2013) Pro-apoptotic miRNA-128-2 modulates ABCA1, ABCG1 and RXRα expression and cholesterol homeostasis. Cell Death Dis 4:e780.

Al Tanoury Z, Piskunov A, Rochette-Egly C (2013) Vitamin A and retinoid signaling: genomic and nongenomic effects. J Lipid Res 54:1761-1775.

Aoto J, Nam CI, Poon MM, Ting P, Chen L (2008) Synaptic signaling by all-trans retinoic acid in homeostatic synaptic plasticity. Neuron 60:308-320.

Carter CJ, Farrar N, Carlone RL, Spencer GE (2010) Developmental expression of a molluscan RXR and evidence for its novel, nongenomic role in growth cone guidance. Dev Biol 343:124-137.

Carter C, Clark A, Spencer G, Carlone R (2011) Cloning and expression of a retinoic acid receptor β2 subtype from the adult newt: evidence for an early role in tail and caudal spinal cord regeneration. Dev Dyn 240:2613-2625.

Carter CJ, Rand C, Mohammad I, Lepp A, Vesprini N, Wiebe O, Carlone R, Spencer GE (2015) Expression of a retinoic acid receptor (RAR)-like protein in the embryonic and adult nervous system of a protostome species. J Exp Zool B Mol Dev Evol 324:51-67.

Chen N, Onisko B, Napoli JL (2008) The nuclear transcription factor RARα associates with neuronal RNA granules and suppresses translation. J Biol Chem 283:20841-20847.

Corcoran J, Shroot B, Pizzey J, Maden M (2000) The role of retinoic acid receptors in neurite outgrowth from different population of embryonic mouse dorsal root ganglia. J Cell Sci 113:2567-2574.

Corcoran J, So PL, Barber RD, Vincent KJ, Mazarakis ND, Mitrophanous KA, Kingsman SM, Maden M (2002) Retinoic acid receptor β2 and neurite outgrowth in the adult mouse spinal cord in vitro. J Cell Sci 115:3779-3786.

Cunningham TJ, Duester G (2015) Mechanisms of retinoic acid signalling and its roles in organ and limb development. Nat Rev Mol Cell Biol 16:110-123.

Di Masi A, Leboffe L, De Marinis E, Pagano F, Cicconi L, Rochette-Egly C, Lo-Coco F, Ascenzi P, Nervi C (2015). Retinoic acid receptors: from molecular mechanisms to cancer therapy. Mol Aspects Med 41:1-115.

Dmetrichuk JM, Spencer GE, Carlone RL (2005) Retinoic acid-dependent attraction of adult spinal cord axons towards regenerating newt limb blastemas in vitro. Dev Biol 281:112-120.

Dollé P (2009) Developmental expression of retinoic acid receptors (RARs). Nucl Recept Signal 7:e006.

Duester G (2013) Retinoid signaling in control of progenitor cell differentiation during mouse development. Semin Cell Dev Biol 24:694-700.

Goncalves MB, Malmqvist T, Clarke E, Hubens CJ, Grist J, Hobbs C, Carlstedt TP, Corocoran JP (2015) Neuronal RARβ signaling modulates PTEN activity directly in neurons and via exosome transfer in astrocytes to prevent glial scar formation and induce spinal cord regeneration. J Neurosci 35:15731-15745.

Iten LE, Bryant SV (1973) Forelimb regeneration from different levels of amputation in the newt, Notophthalmus viridescens: length, rate, and stages. Wilhelm Roux Arch Entwickl Mech Org 173:263-282.

Iten LE, Bryant SV (1976) Stages of tail regeneration in the adult newt, Notophthalmus viridescens. J Exp Zool 196:283-292.

Ji J, Zhang J, Huang G, Qian J, Wang X, Mei S (2009) Over-expressed microRNA-27a and 27b influence fat accumulation and cell proliferation during rat hepatic stellate cell activation. FEBS Lett 583:759-766.

Krezel W, Kastner P, Chambon P (1999) Differential expression of retinoid receptors in the adult mouse central nervous system. Neuroscience 89:1291-1300.

Lefebvre P, Benomar Y, Staels B (2010) Retinoid X receptors: common heterodimerization partners with distinct functions. Trends Endocrinol Metab 21:676-683.

Leid M, Kastner P, Lyons R, Nakshatri H, Saunders M, Zacharewski T, Chen JY, Staub A, Garnier JM, Mader S, Chambon P (1992) Purification, cloning, and RXR identity of the HeLa cell factor with which RAR or TR heterodimerizes to bind target sequences efficiently. Cell 68:377-395.

Liu K, Tedeschi A, Park KK, He Z (2011) Neuronal intrinsic mechanisms of axon regeneration. Annu Rev Neurosci 34:131-152.

Luria A, Furlow JD (2004) Spatiotemporal retinoid-X receptor activation detected in live vertebrate embryos. Proc Natl Acad Sci U S A 101:8987-8992.

Maden M (2002) Retinoid signalling in the development of the central nervous system. Nat Rev Neurosci 3:843-853.

Maden M (2007) Retinoic acid in the development, regeneration and maintenance of the nervous system. Nat Rev Neurosci 8:755-765.

Maghsoodi B, Poon MM, Nam CI, Aoto J, Ting P, Chen L (2008) Retinoic acid regulates RARα-mediated control of translation in dendritic RNA granules during homeostatic synaptic plasticity. Proc Natl Acad Sci U S A 105:16015-16020.

Mangelsdorf DJ, Borgmeyer U, Heyman RA, Zhou JY, Ong ES, Oro AE, Kakizuka A, Evans RM (1992) Characterization of three RXR genes that mediate the action of 9-cis retinoic acid. Genes Dev 6:329-344.

Mark M, Ghyselinck, NB, Chambon P (2009) Function of retinoic acid receptors during embryonic development. Nucl Recept Signal 7:e002

Nickkho-Amiry M, McVey R, Holland C (2012) Peroxisome proliferator-activated receptors modulate proliferation and angiogenesis in human endometrial carcinoma. Mol Cancer Res 10:441-453.

Nguyen M, Singhal P, Piet JW, Shefelbine SJ, Maden M, Voss SR, Monaghan JR (2017) Retinoic acid receptor regulation of epimorphic and homeostatic regeneration in the axolotl. Development 144:601-611.

Piskunov A, Al Tanoury Z, Rochette-Egly C (2014) Nuclear and extra-nuclear effects of retinoid acid receptors: how they are interconnected. Subcell Biochem 70:103-127.

Rand CD, Spencer GE, Carlone RL (2017) Retinoic acid as a chemoattractant for cultured embryonic spinal cord neurons of the African Clawed Frog, Xenopus laevis. Can J Zool 95:653-661.

Reddien PW, Tanaka EM (2016) Editorial overview: Cell reprogramming, regeneration and repair. Curr Opin Genet Dev 40:iv-vi.

Sánchez Alvarado A, Tsonis PA (2006) Bridging the regeneration gap: genetic insights from diverse animal models. Nat Rev Genet 7:873-884.

Schrage K, Koopmans G, Joosten EA, Mey J (2006) Macrophages and neurons are targets of retinoic acid signaling after spinal cord contusion injury. Eur J Neurosci 23:285-295.

Silver J, Miller JH (2004) Regeneration beyond the glial scar. Nat Rev Neurosci 5:146-156.

Simandi Z, Horvath A, Cuaranta-Monroy I, Sauer S, Deleuze JF, Nagy L (2017) RXR heterodimers orchestrate transcriptional control of neurogenesis and cell fate specification. Mol Cell Endocrinol doi: 10.1016/j.mce.2017.07.033.

Solomin L, Johansson CB, Zetterström RH, Bissonnette RP, Heyman RA, Olson L, Lendahl U, Frisén J, Perlmann T (1998) Retinoid-X receptor signalling in the developing spinal cord. Nature 395:398-402.

Tanaka EM, Ferretti P (2009) Considering the evolution of regeneration in the central nervous system. Nat Rev Neurosci 10:713-723.

Tsai EM, Wang YC, Lee TT, Tsai CF, Lai FJ, Yokoyama KK, Hsieh TH, Wu RM, Lee, JN (2015) Dynamic Trk and G Protein signaling regulate dopaminergic neurodifferentiation in human trophoblast stem cells. PLoS One 10:e0143852.

van Neerven S, Mey J (2007) RAR/RXR and PPAR/RXR signaling in spinal cord injury. PPAR Res 2007:29275.

Wong LF, Yip PK, Battaglia A, Grist J, Corcoran J, Maden M, Azzouz M, Kingsman SM, Kingsman AJ, Mazarakis ND, McMahon SB (2006) Retinoic acid receptor β2 promotes functional regeneration of sensory axons in the spinal cord. Nat Neurosci 9:243-250.

Yip PK, Wong LF, Pattinson D, Battaglia A, Grist J, Bradbury EJ, Maden M, McMahon SB, Mazarakis ND (2006) Lentiviral vector expressing retinoic acid receptor β2 promotes recovery of function after corticospinal tract injury in the adult rat spinal cord. Hum Mol Genet 15:3107-3118.

Zhelyaznik N, Mey J (2006) Regulation of retinoic acid receptors α, β and retinoid X receptor α after sciatic nerve injury. Neuroscience 141:1761-1774.

Zukor KA, Kent DT, Odelberg SJ (2011) Meningeal cells and glia establish a permissive environment for axon regeneration after spinal cord injury in newts. Neural Dev 6:1.